JACS
JOURNAL OF THE AMERICAN CHEMICAL SOCIETY
Communication
pubs.acs.org/JACS

Encapsulation of a Metal–Organic Polyhedral in the Pores of a Metal–Organic Framework

Xuan Qiu, Wei Zhong, Cuihua Bai, and Yingwei Li*

School of Chemistry and Chemical Engineering, South China University of Technology, Guangzhou 510640, China

Supporting Information

ABSTRACT: A new and efficient hydrophilicity-directed approach (HDA) is developed to encapsulate large guest molecules beyond the aperture size limitation in the nanospace of metal–organic frameworks (MOFs), as exemplified by the self-assembly of a metal–organic polyhedral (MOP) M_6L_4 into MIL-101. This strategy is based on the different hydrophilicities between inner and outer surfaces of the preformed MOF that may direct the self-assembly of the MOP in the MOF pores by using a two-solvent system. Importantly, as the MOP guest molecule is larger than the MOF aperture size, aggregation and leaching are effectively prevented, endowing the encapsulated MOP with significantly enhanced reactivity and stability in the catalytic transformations as compared to the pristine MOP.

Metal–organic polyhedrals (MOPs) are a newly developed class of inorganic–organic discrete coordination complexes, which are usually prepared by self-assembly of metal ions and highly directional and functionalized ligands.[1] Due to the tailored structure and special symmetry, MOPs experienced rapid development in recent years and have exhibited a wide range of applications such as molecular flasks or molecular recognizers.[2a−c] As one of the most representative MOPs, M_6L_4 features an octahedral self-assembly (Scheme 1a).[1l,3] Although this MOP has some unique advantages such as being highly water-soluble and commercially available, its application is limited to molecular sensing or photocatalysis under mild conditions.[2a−c,4] This limitation is mostly associated with the instability of MOPs, which tend to aggregate under relatively harsh reaction conditions (such as high temperatures).[2d,e] Encapsulation of an MOP into the cavity of a host with windows smaller than the MOP could circumvent this problem and, thus, greatly broaden the application scope of MOPs.

Scheme 1. Preparation of M_6L_4 (a) and M_6L_4⊂MIL-101 (b)

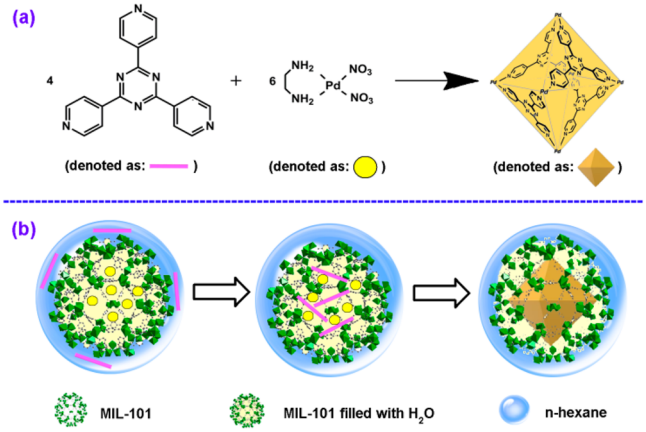

Metal–organic frameworks (MOFs) are a new class of porous materials.[5] Particularly, the well-defined and functionalizable pores may provide accommodative spaces, making MOFs one type of the most promising candidates for the encapsulation of various guests (e.g., metal nanoparticles, organometallic complexes, and polyoxometallate).[6] The great structural and chemical tunability of MOFs have led to a variety of methodologies for the preparation of such host–guest composites by incorporating a guest molecule as an entity, such as impregnation,[7a,b] chemical vapor deposition,[7c,d] and cation exchange,[7e] endowing the composites with excellent performance in catalysis, gas adsorption, etc.[8] Despite the success, these methods are usually restricted by the MOF aperture size, resulting in inaccessibility for larger guest molecules. Coassembly of the guest during MOF crystal growth offers a solution to this problem. However, it often perturbs MOF growth. Recently, Ma's group developed a new strategy for guest encapsulation into MOFs via metal-cation-directed *de novo* assembly from the component fragments of the guest molecule.[9] More recently, Tsung's group introduced a new concept for incorporating large guest molecules as an entity into MOFs via expanded apertures created by dissociative linker exchange.[10] These strategies might offer new insights into such host–guest system and impart new interest in developing more general and facile approaches for preparation of this type of composites.

Herein, we report a novel hydrophilicity-directed approach (HDA), based on the different hydrophilicities of the guest and host, for the encapsulation of an MOP larger than the MOF aperture size into the MOF pores. The HDA strategy typically includes two steps: (1) introducing a small amount of solvent (I) suitable for MOP assembly into the preformed MOF using a two-solvent system and (2) assembling the metal salts and ligands that are introduced into the MOF pores by dissolution or diffusion to form the MOP.

As a proof of principle, we employed MIL-101(Cr) as the host and M_6L_4 as a model MOP guest, respectively. The MIL-101(Cr), a representative MOF, holds two types of mesopores with internal free diameters of ca. 29 and 34 Å.[11] The smaller one possesses pentagonal windows with a free opening of ∼12 Å,

Received: November 20, 2015
Published: January 20, 2016

DOI: 10.1021/jacs.5b12189
J. Am. Chem. Soc. 2016, 138, 1138−1141

while the larger one owns both pentagonal and hexagonal windows with an aperture of 14.5 and 16 Å, respectively.[11] M_6L_4 is a hollow octahedral self-assembly with a diagonal Pd−Pd distance of 2.2 nm, in which **M** stands for $(en)Pd(NO_3)_2$ and **L** stands for 1,3,5-Tris(4-pyridyl)-2,4,6-triazine (TPT).[3] In this complex, the six vertices of the octahedron are occupied by cationic **M**, whereas the eight triangular faces are alternately occupied by four *exo*-tridentate triangular ligands **L** (Scheme 1a).[3] As the pore windows of MIL-101(Cr) are smaller than M_6L_4, the migration and leaching of M_6L_4 could be effectively prohibited if it is encapsulated in the MOF pore.

The synthesis process by using the HDA strategy is illustrated in Scheme 1b. Typically, activated MIL-101 and **L** were first added into a large amount of *n*-hexane, and then a small amount of aqueous **M** solution ($V_{solution} < V_{pore\ of\ MOF}$) was added. As the MIL-101 inner surface was more hydrophilic than the outer surface, the small amount of aqueous **M** solution was readily incorporated into the MIL-101 pores by capillary force.[12] Thus, MIL-101 was suspended in *n*-hexane with pores filled with aqueous **M** solution. Because M_6L_4 was easily self-assembled in water,[3] **L** was drawn into the MIL-101 pores due to the chemical equilibrium shift of the self-assembly process of forming M_6L_4.

The obtained materials were subsequently washed with a large quantity of deionized water until no Pd traces could be detected in the filtrate. This operation was performed carefully in order to exclude the influence of the absorbed Pd species on the MOF surface. Finally, the hybrids were activated by heating at 150 °C for 12 h under dynamic vacuum. The as-synthesized materials are denoted as M_6L_4⊂MIL-101-*N* (*N* = 3, 4, 6, or 10), where *N* represents the average number of MOF cavities that accommodate one M_6L_4 in theory, according to the amount of the precursors added in the reaction solution. The actual Pd contents doped in the MOF were measured by Atomic Absorption Spectroscopy (AAS), showing a high doping efficiency (ca. 90%) of Pd (Table S1).

The crystallinity of the M_6L_4⊂MIL-101 materials was examined by powder X-ray diffraction (PXRD). As shown in Figure S1, the PXRD patterns of M_6L_4⊂MIL-101 hybrids were similar to the parent MIL-101,[11] demonstrating the well preservation of crystalline structure during the incorporation process.

The successful incorporation of M_6L_4 on the MOF was confirmed by NMR spectroscopy taking M_6L_4⊂MIL-101-4 as an example. The liquid ^1H NMR spectrum of pure M_6L_4 was shown in Figure S2, which was consistent with the literature report.[3] However, the solid-state NMR spectra of M_6L_4 have never been reported. In this work, the ^{13}C solid-state NMR spectrum of M_6L_4 (Figures 1a and S3) showed principally five peaks. The signals at δ = 168.99, 153.26, 143.57, and 124.90 ppm were characteristic peaks of **L**, while the peak located at δ = 48.65 ppm corresponded to the ethanediamine group in **M**. In contrast, the parent MIL-101 showed no obvious NMR signal because MIL-101 contains paramagnetic Cr centers. The strong dipolar interactions between the unpaired electrons of the paramagnetic Cr centers and the NMR-active nuclei accelerate nuclear spin relaxation and shift NMR signals, making some signals "invisible".[13] As expected, the M_6L_4⊂MIL-101−4 (Figure 1a) also showed the characteristic peaks of M_6L_4. The peaks intensity was much lower than the pristine M_6L_4 due to the low content of M_6L_4 confined in the hybrid. These results demonstrated that M_6L_4 was successfully synthesized and doped on the MIL-101. Additionally, no obvious chemical shifts were observed, indicating the structural and chemical properties of M_6L_4 were not perturbed during the M_6L_4⊂MIL-101 synthesis process.

The incorporation of M_6L_4 on MIL-101 was further confirmed by Fourier Transform infrared spectroscopy (FT-IR). As presented in Figure 1b, the spectrum of M_6L_4⊂MIL-101-4 exhibited characteristic bonds of both M_6L_4 and MIL-101. Noteworthy, the peaks at 1061 cm^{-1} were assigned to C−N stretching in the **L**. No obvious shifts were also observed between the M_6L_4⊂MIL-101-4 and pristine M_6L_4, indicating that the M_6L_4 in MIL-101 pores preserved its original structure and property. The characteristic framework −(O−C−O)− band at ca. 1400 cm^{-1} was broadened obviously and slightly shifted after M_6L_4 incorporation, suggesting possible encapsulation of M_6L_4 in the MIL-101 pores.

TEM, high-angle annular dark-field scanning transmission electron microscopy (HAADF-STEM), and energy dispersive X-ray spectroscopy (EDS) elemental mapping analyses of M_6L_4⊂MIL-101-4 showed no distinctly congregated Pd particles, demonstrating a uniform distribution of M_6L_4 in the MOF (Figures S4a and S5a−c). The HAADF-STEM and elemental mapping images (Figures 2 and S6) of the ultrathin slices from M_6L_4⊂MIL-101-4 confirmed that Cr and Pd elements were distributed homogeneously, indicating that M_6L_4 was uniformly dispersed in the MIL-101 cavities. Moreover, scanning electron microscopy (SEM) and EDS

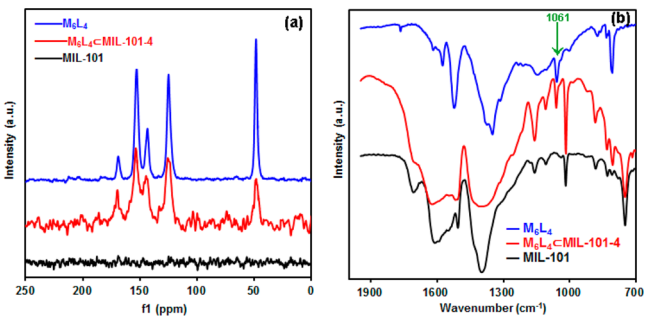

Figure 1. Solid-state ^{13}C NMR spectra (a), and FT-IR spectra (b) of the materials.

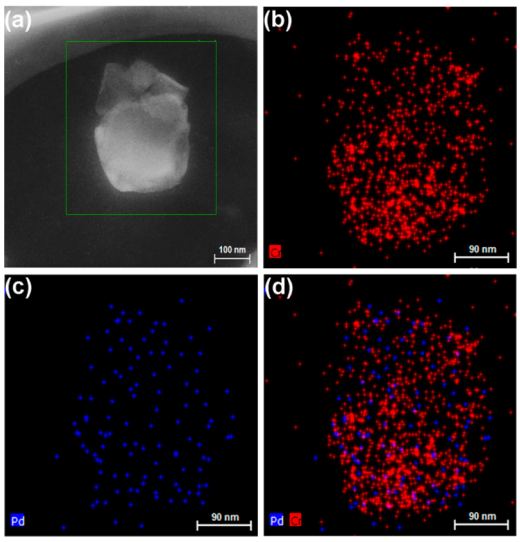

Figure 2. HAADF-STEM image of ultrathin cuts from M_6L_4⊂MIL-101-4 (a), and the corresponding elemental mapping images of Cr (b), Pd (c), and Cr + Pd (d).

DOI: 10.1021/jacs.5b12189
J. Am. Chem. Soc. 2016, 138, 1138−1141

elemental mapping analyses (Figure S7) also revealed an even distribution of Cr, Pd, and N all over the octahedral crystals. These measurements indicated that the M_6L_4 was homogeneously distributed in the MIL-101 pores without the presence of neither accumulation in a particular region nor clusters of bulk M_6L_4 that were physically mixed with the parent MOF.

To investigate the potential interactions between M_6L_4 and MIL-101, we further characterized the materials by X-ray photoelectron spectroscopy (XPS). N and Pd elements were presented obviously in the composites as shown by the XPS survey spectrum of M_6L_4⊂MIL-101-4 (Figures 3c and S8). The

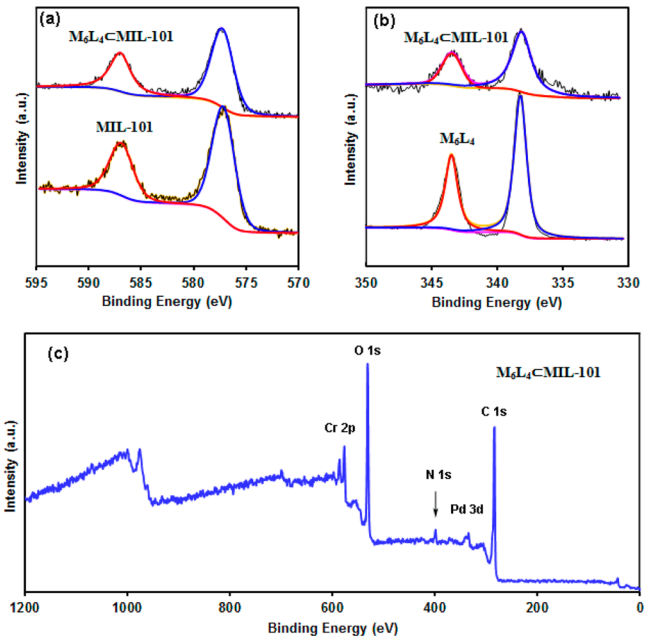

Figure 3. Cr 2p (a) and Pd 3d (b) XPS spectra of M_6L_4⊂MIL-101-4, MIL-101, and M_6L_4. Survey spectrum of M_6L_4⊂MIL-101-4 (c).

Pd XPS spectra of both M_6L_4 and M_6L_4⊂MIL-101-4 (Figure 3b) exhibited Pd $3d_{5/2}$ bands at ca. 338.3 eV and Pd $3d_{3/2}$ bands at ca. 343.6 eV, typical characteristics of Pd(II) ions.[14] No appreciable differences were observed in the binding energies of the Pd(3d) spectra for the two materials. Similarly, there was no apparent shift between the Cr binding energies for the M_6L_4⊂MIL-101-4 and MIL-101 (Figure 3a). These observations suggested that no strong electron interaction between the M_6L_4 and MIL-101 was present in the composites.

The surface areas and porosities of the hybrids were measured by N_2 adsorption at 77 K. The M_6L_4⊂MIL-101 samples (Figure S9) all showed type I isotherms similar to that of the parent MIL-101, indicating that the M_6L_4⊂MIL-101 materials still maintained the porous structure of MIL-101. In comparison with the parent MIL-101, obvious decreases in the BET surface areas and pore volumes (Table S2) were observed due to the occupation of the pores, further confirming the incorporation of M_6L_4 within the MIL-101 pores.[9,10] As the content of M_6L_4 increased, the BET surface areas and pore volumes of M_6L_4⊂MIL-101 decreased gradually as expected.

To elucidate the advantages of our HDA assembly strategy for the encapsulation of MOP in MOFs, two traditional methods were also attempted for the incorporation of M_6L_4 into MIL-101. The obtained materials are named as M_6L_4/MIL-101 and M_6L_4@MIL-101, respectively. For the preparation of M_6L_4/MIL-101 by impregnation, MIL-101 particles were directly soaked in the M_6L_4 aqueous solution. The impregnation approach was not efficient for M_6L_4 incorporation as evidenced by the extremely low M_6L_4 loading (Table S1; Figures S10–S11). Moreover, HAADF-STEM images (Figure S12a) showed that M_6L_4 was aggregated on the MOF surface. The attempt to encapsulate M_6L_4 into MIL-101 employing only one solvent, i.e., soaking MIL-101 in the **M** and **L** mixed aqueous solution, did not succeed either (Table S1; Figures S13–S14). Additionally, leaching experiments showed that M_6L_4/MIL-101 and M_6L_4@MIL-101 underwent obvious Pd leaching while M_6L_4⊂MIL-101 did not show any significant loss of Pd (Table S3). These comparisons highlighted the effectiveness of the HDA strategy for encapsulating large MOP molecules into the pores of MOFs.

To demonstrate that the HDA strategy can enhance the stability and performance of the MOP confined in the MOF, we examined the catalytic property of the M_6L_4⊂MIL-101 hybrids in the selective oxidation of benzyl alcohol to benzaldehyde (Figure 4 and Table S4). The blank reactions without a catalyst or even

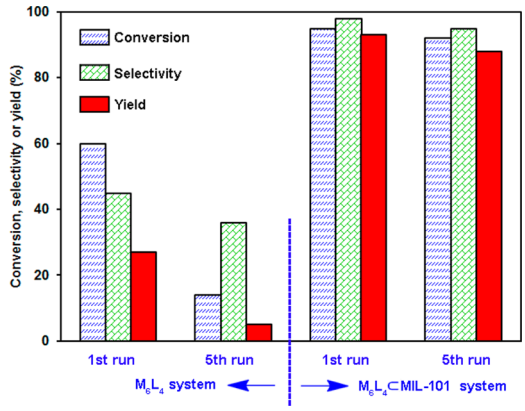

Figure 4. Catalytic performance and reusability of the M_6L_4 and M_6L_4⊂MIL-101–4 materials in benzyl alcohol oxidation.

with MIL-101 gave essentially no conversions (<5%) at 130 °C for 18 h. M_6L_4 exhibited some reactivity and afforded 60% conversion with 45% selectivity to benzaldehyde after 18 h of reaction (Figure 4), with benzoic acid and benzyl benzoate as the main side products. In comparison, the M_6L_4⊂MIL-101-4 showed significantly improved activity and selectivity, giving 98% selectivity to benzaldehyde at 95% conversion under identical conditions. As compared to M_6L_4, it was impressive that the benzaldehyde yield was enhanced by a factor of ca. 3.5. More importantly, the catalytic activity and selectivity of M_6L_4⊂MIL-101-4 remained almost unchanged even after five reuses, while the pristine M_6L_4 deactivated dramatically (Figure 4). As a consequence, the benzaldehyde yield obtained on the M_6L_4⊂MIL-101-4 system was nearly 20 times higher than that of M_6L_4 after being reused five times. Both M_6L_4@MIL-101 and M_6L_4/MIL-101 showed significantly inferior catalytic performance compared to M_6L_4⊂MIL-101-4. A possible reaction mechanism was proposed in Scheme S1.

The stability of M_6L_4⊂MIL-101-4 was confirmed by TEM and HAADF-STEM measurements, which showed no obvious catalyst aggregation after recycling (Figures S4b and S5d–i). XPS measurements of the recovered M_6L_4⊂MIL-101-4 indicated that palladium remained in its divalent form (Figure S15). The well preservation of the M_6L_4⊂MIL-101-4 structure after reactions was further demonstrated by FT-IR analysis, which showed a spectrum almost identical to the fresh one (Figure

DOI: 10.1021/jacs.5b12189
J. Am. Chem. Soc. 2016, 138, 1138–1141

S16). However, the M_6L_4 system encountered serious catalyst degradation during reaction, in which palladium aggregates with diameters of 5−20 nm were clearly observed even only after the first run (Figure S4d). The remarkably enhanced reactivity and stability of M_6L_4⊂MIL-101-4 as compared to M_6L_4 is believed to be related to the encapsulation effect offered by the MOF cavities, featuring highly dispersed M_6L_4 active centers without any significant leaching or aggregation.

In summary, we have developed, for the first time, a hydrophilicity-directed approach (HDA) for the encapsulation of an MOP into MOFs beyond the framework aperture size limitation, as exemplified by the self-assembly of M_6L_4 into MIL-101. The confined M_6L_4 exhibited significantly improved catalytic efficiency and stability compared with the pristine MOP material. The HDA strategy requires neither particular types of MOFs nor destruction of the MOFs, thus offering a versatile approach to encapsulating a broad range of MOP complexes into MOFs with significantly enhanced performance for various applications. Studies aimed at extending this strategy to the encapsulation of other types of MOPs into MOFs for advanced catalysis applications are currently underway in our laboratory.

■ ASSOCIATED CONTENT

Supporting Information

The Supporting Information is available free of charge on the ACS Publications website at DOI: 10.1021/jacs.5b12189.

Procedures and additional data (PDF)

■ AUTHOR INFORMATION

Corresponding Author

*liyw@scut.edu.cn

Notes

The authors declare no competing financial interest.

■ ACKNOWLEDGMENTS

We thank the National NSF of China (21322606, 21436005, and 21576095), the Doctoral Fund of Ministry of Education of China (20120172110012), Fundamental Research Funds for the Central Universities (2015ZP002 and 2015PT004), and Guangdong NSF (2013B090500027) for financial support.

■ REFERENCES

(1) (a) Stang, P. J.; Olenyuk, B. *Acc. Chem. Res.* **1997**, *30*, 502. (b) Leininger, S.; Olenyuk, B.; Stang, P. J. *Chem. Rev.* **2000**, *100*, 853. (c) Cook, T. R.; Zheng, Y.; Stang, P. J. *Chem. Rev.* **2013**, *113*, 734. (d) Seidel, S. R.; Stang, P. J. *Acc. Chem. Res.* **2002**, *35*, 972. (e) Northrop, B. H.; Zheng, Y.; Chi, K.-W.; Stang, P. J. *Acc. Chem. Res.* **2009**, *42*, 1554. (f) Fujita, M. *Chem. Soc. Rev.* **1998**, *27*, 417. (g) Chakrabarty, R.; Mukherjee, P. S.; Stang, P. J. *Chem. Rev.* **2011**, *111*, 6810. (h) Yoshizawa, M.; Klosterman, J. K.; Fujita, M. *Angew. Chem., Int. Ed.* **2009**, *48*, 3418. (i) Klosterman, J. K.; Yamauchi, Y.; Fujita, M. *Chem. Soc. Rev.* **2009**, *38*, 1714. (j) Ahmad, N.; Chughtai, A. H.; Younus, H. A.; Verpoort, F. *Coord. Chem. Rev.* **2014**, *280*, 1. (k) Koblenz, T. S.; Wassenaar, J.; Reek, J. N. H. *Chem. Soc. Rev.* **2008**, *37*, 247. (l) Vardhan, H.; Verpoort, F. *Adv. Synth. Catal.* **2015**, *357*, 1351. (m) Han, Y.; Li, J.; Xie, Y.; Guo, G. *Chem. Soc. Rev.* **2014**, *43*, 5952. (n) Ramsay, W. J.; Szczypiński, F. T.; Weissman, H.; Ronson, T. K.; Smulders, M. M.; Rybtchinski, B.; Nitschke, J. R. *Angew. Chem., Int. Ed.* **2015**, *54*, 5636. (o) Perry, J. J., IV; Perman, J. A.; Zaworotko, M. J. *Chem. Soc. Rev.* **2009**, *38*, 1400.

(2) (a) Ahmad, N.; Younus, H. A.; Chughtai, A. H.; Verpoort, F. *Chem. Soc. Rev.* **2015**, *44*, 9. (b) Kohyama, Y.; Murase, T.; Fujita, M. *J. Am. Chem. Soc.* **2014**, *136*, 2966. (c) Roukala, J.; Zhu, J.; Giri, C.; Rissanen, K.; Lantto, P.; Telkki, V. V. *J. Am. Chem. Soc.* **2015**, *137*, 2464. (d) Sun, L.; Li, J.; Lu, W.; Gu, Z.; Luo, Z.; Zhou, H. *J. Am. Chem. Soc.* **2012**, *134*, 15923. (e) Lu, W.; Yuan, D.; Yakovenko, A.; Zhou, H. *Chem. Commun.* **2011**, *47*, 4968.

(3) (a) Fujita, M.; Oguro, D.; Miyazawa, M.; Oka, H.; Yamaguchi, K.; Ogura, K. *Nature* **1995**, *378*, 469. (b) Fujita, M.; Tominaga, M.; Hori, A.; Therrien, B. *Acc. Chem. Res.* **2005**, *38*, 369. (c) Fujita, M.; Yoshizawa, M. *New properties and reactions in self-assembled M_6L_4 coordination cages*; Wiley-VCH Verlag GmbH & Co. KGaA: Weinheim, Germany, 2008; p 277.

(4) (a) Yamaguchi, T.; Fujita, M. *Angew. Chem., Int. Ed.* **2008**, *47*, 2067. (b) Horiuchi, S.; Murase, T.; Fujita, M. *J. Am. Chem. Soc.* **2011**, *133*, 12445.

(5) (a) Furukawa, H.; Cordova, K. E.; O'Keeffe, M.; Yaghi, O. M. *Science* **2013**, *341*, 974. (b) Li, J.; Sculley, J.; Zhou, H. *Chem. Rev.* **2012**, *112*, 869. (c) Cohen, S. M. *Chem. Rev.* **2012**, *112*, 970. (d) Colón, Y. J.; Snurr, R. Q. *Chem. Soc. Rev.* **2014**, *43*, 5735. (e) Zhang, W.; Liu, Y.; Lu, G.; Wang, Y.; Li, S.; Cui, C.; Wu, J.; Xu, Z.; Tian, D.; Huang, W.; DuCheneu, J. S.; Wei, W.; Chen, H.; Yang, Y.; Huo, F. *Adv. Mater.* **2015**, *27*, 2923.

(6) (a) Dhakshinamoorthy, A.; Garcia, H. *Chem. Soc. Rev.* **2012**, *41*, 5262. (b) Moon, H. R.; Lim, D. W.; Suh, M. P. *Chem. Soc. Rev.* **2013**, *42*, 1807. (c) Valvekens, P.; Vermoortele, F.; De Vos, D. *Catal. Sci. Technol.* **2013**, *3*, 1435. (d) Hermannsdörfer, J.; Friedrich, M.; Miyajima, N.; Albuquerque, R. Q.; Kümmel, S.; Kempe, R. *Angew. Chem., Int. Ed.* **2012**, *51*, 11473. (e) Hu, P.; Morabito, J. V.; Tsung, C. K. *ACS Catal.* **2014**, *4*, 4409. (f) Zhao, M.; Deng, K.; He, L.; Liu, Y.; Li, G.; Zhao, H.; Tang, Z. *J. Am. Chem. Soc.* **2014**, *136*, 1738. (g) Li, Y.; Tang, J.; He, L.; Liu, Y.; Liu, Y.; Chen, C.; Tang, Z. *Adv. Mater.* **2015**, *27*, 4075. (h) Pascanu, V.; Gómez, A. B.; Ayats, C.; Platero-Prats, A. E.; Carson, F.; Su, J.; Yao, Q.; Pericàs, M. À.; Zou, X.; Martín-Matute, B. *ACS Catal.* **2015**, *5*, 472. (i) Na, K.; Choi, K. M.; Yaghi, O. M.; Somorjai, G. A. *Nano Lett.* **2014**, *14*, 5979. (j) Nepal, B.; Das, S. *Angew. Chem., Int. Ed.* **2013**, *52*, 7224. (k) Hansen, R. E.; Das, S. *Energy Environ. Sci.* **2014**, *7*, 317. (l) Zheng, S.-T.; Zhao, X.; Lau, S.; Fuhr, A.; Feng, P.; Bu, X. *J. Am. Chem. Soc.* **2013**, *135*, 10270. (m) Li, J.; Yu, J.; Lu, W.; Sun, L.; Sculley, J.; Balbuena, P. B.; Zhou, H. C. *Nat. Commun.* **2013**, *4*, 1538.

(7) (a) Corma, A.; García, H.; Llabrés i Xamena, F. X. *Chem. Rev.* **2010**, *110*, 4606. (b) Kockrick, E.; Lescouet, T.; Kudrik, E. V.; Sorokin, A. B.; Farrusseng, D. *Chem. Commun.* **2011**, *47*, 1562. (c) Mondloch, J. E.; Bury, W.; Fairen-Jimenez, D.; Kwon, S.; DeMarco, E. J.; Weston, M. H.; Sarjeant, A. A.; Nguyen, S. T.; Stair, P. C.; Snurr, R. Q.; Farha, O. K.; Hupp, J. T. *J. Am. Chem. Soc.* **2013**, *135*, 10294. (d) Hermes, S.; Schröder, F.; Amirjalayer, S.; Schmid, R.; Fischer, R. A. *J. Mater. Chem.* **2006**, *16*, 2464. (e) Genna, D. T.; Wong-Foy, A. G.; Matzger, A. J.; Sanford, M. S. *J. Am. Chem. Soc.* **2013**, *135*, 10586.

(8) (a) Yu, J.; Cui, Y.; Wu, C.; Yang, Y.; Wang, Z.; O'Keeffe, M.; Chen, B.; Qian, G. *Angew. Chem., Int. Ed.* **2012**, *51*, 10542. (b) Larsen, R. W.; Wojtas, L. *J. Mater. Chem. A* **2013**, *1*, 14133. (c) Juan-Alcañiz, J.; Gascon, J.; Kapteijn, F. *J. Mater. Chem.* **2012**, *22*, 10102.

(9) Li, B. Y.; Zhang, Y. M.; Ma, D. X.; Ma, T. L.; Shi, Z.; Ma, S. Q. *J. Am. Chem. Soc.* **2014**, *136*, 1202.

(10) Morabito, J. V.; Chou, L.; Li, Z.; Manna, C. M.; Petroff, C. A.; Kyada, R. J.; Palomba, J. M.; Byers, J. A.; Tsung, C.-K. *J. Am. Chem. Soc.* **2014**, *136*, 12540.

(11) Férey, G.; Mellot-Draznieks, C.; Serre, C.; Millange, F.; Dutour, J.; Surblé, S.; Margiolaki, I. *Science* **2005**, *309*, 2040.

(12) (a) Zhu, Q.; Li, J.; Xu, Q. *J. Am. Chem. Soc.* **2013**, *135*, 10210. (b) Aijaz, A.; Karkamkar, A.; Choi, Y. J.; Tsumori, N.; Rönnebro, E.; Autrey, T.; Shioyama, H.; Xu, Q. *J. Am. Chem. Soc.* **2012**, *134*, 13926.

(13) Čendak, T.; Žunkovič, E.; Godec, T. U.; Mazaj, M.; Logar, N. Z.; Mali, G. *J. Phys. Chem. C* **2014**, *118*, 6140.

(14) (a) Chen, L.; Rangan, S.; Li, J.; Jiang, H.; Li, Y. W. *Green Chem.* **2014**, *16*, 3978. (b) NIST X-ray Photoelectron Spectroscopy Database, version 3.5, Gaithersburg, 2003, http://srdata.nist.gov/xps/.

DOI: 10.1021/jacs.5b12189
J. Am. Chem. Soc. 2016, 138, 1138−1141